

A new 700 GeV scalar in the LHC data?

Maurizio Consoli,¹ George Rupp,²

¹INFN, Sezione di Catania, I-95123 Catania, Italy

²CeFEMA and CFTP, Instituto Superior Técnico, Universidade de Lisboa, P-1049-001 Lisboa, Portugal

Abstract

As an alternative to the metastability of the electroweak vacuum, resulting from perturbative calculations, one can consider a non-perturbative effective potential which, as at the beginning of the Standard Model, is restricted to the pure Φ^4 sector yet consistent with the known analytical and numerical studies. In this approach, where the electroweak vacuum is now the lowest-energy state, besides the resonance of mass $m_h = 125$ GeV defined by the quadratic shape of the potential at its minimum, the Higgs field should exhibit a second resonance with mass $(M_H)^{\text{Theor}} = 690$ (30) GeV associated with the zero-point energy determining the potential depth. In spite of its large mass, this resonance would couple to longitudinal W s with the same typical strength as the low-mass state at 125 GeV and represent a relatively narrow resonance, mainly produced at LHC by gluon-gluon fusion. In this Letter, we review LHC data suggesting a new resonance of mass $(M_H)^{\text{EXP}} \sim 682$ (10) GeV, with a statistical significance that is far from negligible.

Keywords: Higgs mass spectrum, LHC experiments

DOI: 10.2018/LHEP000001

1. INTRODUCTION

The discovery [1, 2] of a narrow scalar resonance with mass $m_h = 125$ GeV and the phenomenological consistency with the expectations for the Higgs boson have confirmed spontaneous symmetry breaking (SSB) through the Higgs field as a fundamental ingredient of current particle physics. Yet, in our opinion, the present perturbative description of symmetry breaking is not entirely satisfactory. Indeed, once we start to look farther than the Fermi scale, such a calculation predicts that the effective potential of the Standard Model (SM) should have a new minimum, well beyond the Planck scale and being much deeper than the electroweak (EW) vacuum; see e.g. [3, 4]. While it is reassuring that the most accurate calculation [5] gives a tunnelling time that is larger than the age of the universe, still the idea of a metastable vacuum raises several questions: the role of gravitational effects, the mechanism explaining why the theory remains trapped in our EW vacuum, This would require a cosmological perspective and to control the properties of matter in the extreme conditions of the early universe.

As an alternative, one can consider [6, 7, 8, 9] a non-perturbative effective potential which, as at the beginning of the SM, is restricted to the pure Φ^4 sector but is also consistent with the known analytical and numerical studies. In this approach, where the EW vacuum is now the lowest-energy state, besides the resonance of mass $m_h = 125$ GeV defined by the quadratic shape of the potential at its minimum, the Higgs field should exhibit a second resonance with a mass $(M_H)^{\text{Theor}} = 690$ (30) GeV, associated with the zero-point energy (ZPE) determining the potential depth. This large M_H stabilises the potential, because including the ZPEs of all known gauge and fermion fields would now represent just a small radiative correction.¹ Like in the early days of the SM, one could thus adopt the perspective of explaining SSB within the pure scalar sector. Checking this picture then requires to observe the second resonance and its phenomenology.

¹By subtracting quadratic divergences or using dimensional regularisation, the logarithmically divergent terms in the ZPEs of the various fields are proportional to the fourth power of the mass. Thus, in units of the pure scalar term, one finds $(6M_w^4 + 3M_t^4)/M_H^4 \lesssim 0.002$ and $12m_t^4/M_H^4 \lesssim 0.05$.

In this respect, the hypothetical H is not like a regular Higgs boson of 700 GeV, because it would couple to longitudinal W s with the same typical strength as the low-mass state at 125 GeV [6, 7, 8, 9]. In fact, it is $m_h = 125$ GeV (and not $M_H \sim 700$ GeV) which fixes the quadratic shape of the potential and the interaction with the Goldstone bosons. Thus, the large conventional widths $\Gamma(H \rightarrow ZZ + WW) \sim G_F M_H^3$ would be suppressed by the small ratio $(m_h/M_H)^2 \sim 0.032$, leading to the estimates $\Gamma(H \rightarrow ZZ) \sim M_H/(700 \text{ GeV}) \times (1.6 \text{ GeV})$ and $\Gamma(H \rightarrow WW) \sim M_H/(700 \text{ GeV}) \times (3.3 \text{ GeV})$. As such, the heavy H should be a relatively narrow resonance of total width $\Gamma(H \rightarrow \text{all}) = 25 \div 35$ GeV, decaying predominantly to $t\bar{t}$ quark pairs, with a branching ratio of about 70–80%. Due to its small coupling to longitudinal W s, H production through vector-boson fusion (VBF) would also be negligible as compared to gluon-gluon fusion (ggF), which has a typical cross section $\sigma^{\text{ggF}}(pp \rightarrow H) \sim 1100$ (170) fb [14, 15], depending on the QCD and H -mass uncertainties.

After this brief review, in this Letter we will present LHC data suggesting a new resonance in the expected mass and width range, with a non-negligible statistical significance. Partial evidence was already presented in Refs. [10, 11, 12, 13], but in Sec. 2 we will consider a larger data set and also refine the analysis of some final states. Finally, Sec. 3 will contain a summary and our conclusions.

2. EXPERIMENTAL SIGNALS FROM LHC

Having a definite prediction $(M_H)^{\text{Theor}} = 690$ (30) GeV, we will look for signals in the expected region of invariant mass 600–800 GeV, so that local deviations from the background should not be downgraded by the “look elsewhere” effect. In this search, one should also keep in mind that, with the present energy and luminosity of LHC, the second resonance is too heavy to be seen unambiguously in all possible channels. (Recall the $h(125)$ discovery, which initially was producing no signals in the important $b\bar{b}$ and $\tau^+\tau^-$ channels).

Now, with an expected large branching ratio $B(H \rightarrow t\bar{t}) = (70 \div 80)\%$, the natural starting point would be the $t\bar{t}$ channel. However, in the relevant region $m(t\bar{t}) = 620 \div 820$ GeV, CMS measurements [16] give a background cross section $\sigma(pp \rightarrow t\bar{t}) = 107 \pm 7.6$ pb, which is about 100 times larger than the expected signal $\sigma(pp \rightarrow H \rightarrow t\bar{t}) \lesssim 1$ pb. Therefore, in Refs. [10, 11, 12, 13]

E[GeV]	$N_{\text{EXP}}(E)$	$N_{\text{B}}(E)$	$N_{\text{EXP}}(E) - N_{\text{B}}(E)$
560(30)	38 ± 6.16	32.0	6.00 ± 6.16
620(30)	25 ± 5.00	20.0	5.00 ± 5.00
680(30)	26 ± 5.10	13.04	12.96 ± 5.10
740(30)	3 ± 1.73	8.71	-5.71 ± 1.73
800(30)	7 ± 2.64	5.97	1.03 ± 2.64

TABLE 1: For luminosity 139 fb^{-1} , we give the ATLAS ggF-low events $N_{\text{EXP}}(E)$ and the estimated background $N_{\text{B}}(E)$ [17, 18] for invariant mass $m_{4l} = E = 530 \div 830 \text{ GeV}$. To avoid spurious migrations between neighbouring bins, we group the data into bins of 60 GeV, corresponding to the 10 bins of 30 GeV from 545 (15) GeV to 815 (15) GeV; see Ref. [18].

the analysis was focused on available channels with relatively smaller background, namely:

- i) ATLAS ggF-like 4-lepton events;
- ii) ATLAS high-mass inclusive $\gamma\gamma$ events;
- iii) ATLAS and CMS ($b\bar{b} + \gamma\gamma$) events;
- iv) CMS $\gamma\gamma$ pairs produced in pp diffractive scattering.

2.1. The ATLAS ggF-like 4-lepton events

To start with, we will review ATLAS work [17, 18] dedicated to the charged 4-lepton channel and to the search for a heavy scalar resonance H decaying through the chain $H \rightarrow ZZ \rightarrow 4l$. This is important because, for this particular channel, there is a precise prediction characteristic of our picture. Indeed, for a relatively narrow resonance, the resonant peak cross section $\sigma_R(pp \rightarrow H \rightarrow 4l)$ can be well approximated as

$$\sigma_R(pp \rightarrow H \rightarrow 4l) \sim \sigma(pp \rightarrow H) B(H \rightarrow ZZ) 4B^2(Z \rightarrow l^+l^-), \quad (1)$$

with $4B^2(Z \rightarrow l^+l^-) \sim 0.0045$. Thus, in our case, where $\Gamma(H \rightarrow ZZ) \sim M_H/(700 \text{ GeV}) \times (1.6 \text{ GeV})$ and $\sigma(pp \rightarrow H) \sim \sigma^{\text{ggF}}(pp \rightarrow H) \sim 1100 (170) \text{ fb}$, by introducing the reduced width $\gamma_H = \Gamma(H \rightarrow 4l)/M_H$, we find the sharp correlation

$$[\gamma_H \times \sigma_R(pp \rightarrow H \rightarrow 4l)]^{\text{Theor}} \sim (0.011 \pm 0.002) \text{ fb}, \quad (2)$$

to be compared with the ATLAS data.

In the ATLAS search, the 4-lepton events were divided into ggF-like and VBF-like events. By expecting our second resonance to be produced through gluon-gluon fusion, we have considered the ggF-like category. The only sample that satisfies the two requirements, viz. a) being homogeneous from the point of view of the selection and b) having sufficient statistics, is the so called ggF-low category, which contains a mixture of all three final states. Since for an invariant mass around 700 GeV, the energy resolution of these events varies considerably,² it is natural to adopt a large-bin visualisation to avoid spurious fluctuations between adjacent bins. The numbers of events are reported in Table 1 [17, 18].

Now, subtracting the background from the observed events gives a considerable excess, at about 680 GeV, and then a sizable defect, around 740 GeV. A simple explanation for these two simultaneous features would be the existence of a resonance of mass

²The resolution varies from about 12 GeV for $4e$ events to 19 GeV for $2e2\mu$, up to 24 GeV for 4μ .

$M_H \sim 700 \text{ GeV}$ which, above the Breit-Wigner peak, produces the characteristic negative-interference pattern proportional to $(M_H^2 - s)$. To check this idea, we have exploited the basic model where the ZZ pairs, each subsequently decaying into a charged l^+l^- pair, are produced by various mechanisms at the parton level. For $E \equiv m(4l)$, this produces a smooth distribution of background events $N_b(E)$, proportional to a background cross section $\sigma_b(E)$, which can interfere with a resonance of mass M_H and total decay width Γ_H . The total cross section $\sigma_T(E)$ can then be expressed as [8]

$$\sigma_T(E) = \sigma_b(E) + \frac{2(M_H^2 - s)\Gamma_H M_H}{(s - M_H^2)^2 + (\Gamma_H M_H)^2} \sqrt{\sigma_R \sigma_b(E)} + \frac{(\Gamma_H M_H)^2}{(s - M_H^2)^2 + (\Gamma_H M_H)^2} \sigma_R, \quad (3)$$

where we have introduced the resonant peak cross section σ_R at $s = M_H^2$. Then, by simple redefinitions, the theoretical number of events

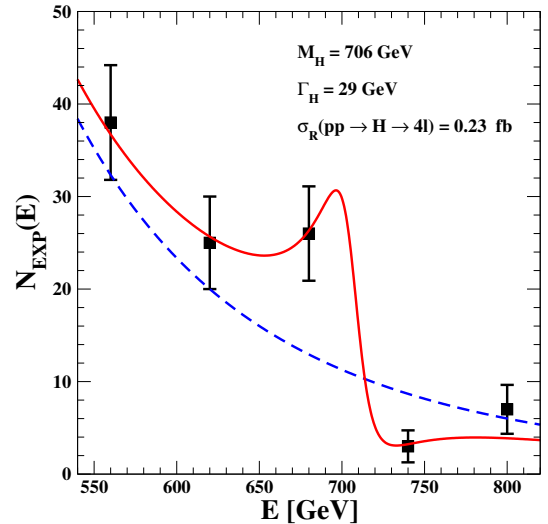


FIGURE 1: The values $N_{\text{EXP}}(E)$ in Table 1 vs. the corresponding $N_{\text{TH}}(E)$ in Eq. (4) (the full red curve). The resonance parameters are $M_H = 706 \text{ GeV}$, $\gamma_H = 0.041$, $\sigma_R = 0.23 \text{ fb}$ and the ATLAS background (dashed blue curve) is approximated as $N_b(E) = A \times (710 \text{ GeV}/E)^\nu$, with $A = 10.55$ and $\nu = 4.72$.

can be expressed as

$$N_{\text{TH}}(E) = N_b(E) + \frac{P^2 + 2P x(E) \sqrt{N_b(E)}}{\gamma_H^2 + x^2(E)}, \quad (4)$$

where $x(E) = (M_H^2 - E^2)/M_H^2$, $P \equiv \gamma_H \sqrt{N_R}$, and $N_R = \sigma_R \mathcal{A} 139 \text{ fb}^{-1}$ denotes the extra events at the resonance peak for an acceptance \mathcal{A} . The data in Table 1 were fitted with Eq. (4) in [12, 13]. The results are: $M_H = 706 (25) \text{ GeV}$, $P = 0.14 \pm 0.07$ and $\gamma_H = 0.041 \pm 0.029$, corresponding to a total width $\Gamma_H = 29 \pm 20 \text{ GeV}$. One thus obtains $N_R \sim 12_{-9}^{+15}$ and for acceptance $\langle \mathcal{A} \rangle \sim 0.38$, by averaging the two extremes 0.30 and 0.46 for the ggF-like category of events [17], $\sigma_R \sim 0.23_{-0.17}^{+0.28} \text{ fb}$. A graphical comparison is shown in Fig. 1.

The quality of the fit is good, but error bars are large and a test of our picture is not very stringent. Still, with our $\Gamma(H \rightarrow ZZ) \sim 1.6 \text{ GeV}$, for $M_H \sim 700 \text{ GeV}$, and the central fitted $\langle \Gamma_H \rangle = 29 \text{ GeV}$, we find a branching ratio $B(H \rightarrow ZZ) \sim 0.055$ which, for the theoretical value $\sigma^{\text{ggF}}(pp \rightarrow H) \sim 923 \text{ fb}$ of Ref. [15]

Bin [GeV]	σ_{EXP} [fb]	σ_{B} [fb]	$(\sigma_{\text{EXP}} - \sigma_{\text{B}})$ [fb]
555–585	0.252 ± 0.056	0.272 ± 0.023	-0.020 ± 0.060
585–620	0.344 ± 0.070	0.259 ± 0.021	$+0.085 \pm 0.075$
620–665	0.356 ± 0.075	0.254 ± 0.023	$+0.102 \pm 0.078$
665–720	0.350 ± 0.073	0.214 ± 0.019	$+0.136 \pm 0.075$
720–800	0.126 ± 0.047	0.206 ± 0.018	-0.080 ± 0.050
800–900	0.205 ± 0.052	0.152 ± 0.017	$+0.053 \pm 0.055$

TABLE 2: The observed ATLAS cross section [19, 20] and estimated background for a 4-lepton invariant mass $m(4l) \equiv E$ from 555 to 900 GeV. These values are obtained by multiplying the bin size with the average differential cross sections $\langle(d\sigma/dE)\rangle$, reported for each bin in the companion HEPData file [20]. The full background cross section σ_{B} contains a dominant contribution from $q\bar{q} \rightarrow 4l$ events.

(at $M_H = 700$ GeV) would imply a theoretical peak cross section $(\sigma_R)^{\text{Theor}} = 923 \times 0.055 \times 0.0045 \sim 0.23$ fb, coinciding with the central value from our fit. Also, from the central values $\langle\sigma_R\rangle = 0.23$ fb and $\langle\gamma_H\rangle = 0.041$, we find $\langle\sigma_R\rangle \langle\gamma_H\rangle \sim 0.0093$ fb, consistent with Eq. (2).

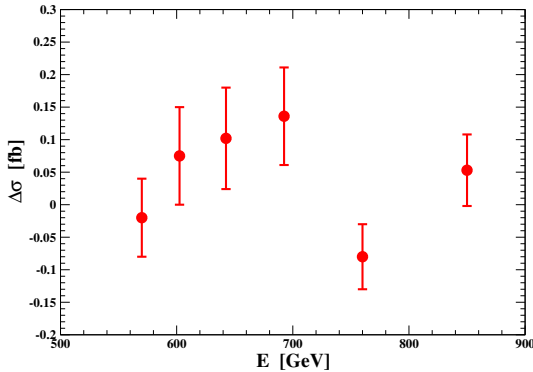


FIGURE 2: The quantity $\Delta\sigma = (\sigma_{\text{EXP}} - \sigma_{\text{B}})$ given for each bin in the last column of Table 2.

After this first comparison from Refs. [12, 13], we will now consider the other ATLAS paper Ref. [19, 20] for the differential 4-lepton cross section $d\sigma/dE$, with $E = m(4l)$. From Fig. 5 of this other Ref. [19], one finds the same excess-defect sequence as in Table 1 and additional support for a new resonance. The corresponding data are given in Table 2 and in Fig. 2. Besides, by comparing with Ref. [19, 20], we can sharpen our analysis. In fact, the ggF-low events considered above contain a large contribution from $q\bar{q} \rightarrow 4l$ processes. Although the initial state is pp in all cases, our H resonance would mainly be produced through gluon-gluon fusion, so that, strictly speaking, the interference should only be computed with the non-resonant $gg \rightarrow 4l$ background. Obtaining this refinement is now possible, because, in Ref. [19, 20], the individual contributions to the background are reported separately. Denoting by $\sigma_{\text{B}}^{\text{gg}}$ the pure non-resonant $gg \rightarrow 4l$ background cross section, we can thus consider a corresponding experimental cross section $\hat{\sigma}_{\text{EXP}}$ after subtracting out preliminarily the “non-ggF” background:

$$\hat{\sigma}_{\text{EXP}} = \sigma_{\text{EXP}} - (\sigma_{\text{B}} - \sigma_{\text{B}}^{\text{gg}}). \quad (5)$$

The corresponding values and background are given in Table 3.

We then compare the resulting experimental $\hat{\sigma}_{\text{EXP}}$ with the theoretical σ_T in Eq. (3), after the identification $\sigma_b = \sigma_{\text{B}}^{\text{gg}}$. By parametrising the ATLAS differential background $(d\sigma_{\text{B}}^{\text{gg}}/dE) \sim A \times (710 \text{ GeV}/E)^{\nu}$, with $A \sim (2.42 \pm 0.18) \times 10^{-4}$ fb/GeV and

Bin [GeV]	$\hat{\sigma}_{\text{EXP}}$ [fb]	$\sigma_{\text{B}}^{\text{gg}}$ [fb]	$(\hat{\sigma}_{\text{EXP}} - \sigma_{\text{B}}^{\text{gg}})$ [fb]
555-585	0.003 ± 0.060	0.023 ± 0.004	-0.020 ± 0.060
585-620	0.105 ± 0.073	0.020 ± 0.003	$+0.085 \pm 0.075$
620-665	0.121 ± 0.078	0.019 ± 0.003	$+0.102 \pm 0.078$
665-720	0.152 ± 0.075	0.016 ± 0.003	$+0.136 \pm 0.075$
720-800	-0.067 ± 0.050	0.013 ± 0.002	-0.080 ± 0.050
800-900	0.062 ± 0.055	0.009 ± 0.002	$+0.053 \pm 0.055$

TABLE 3: For each energy bin, we give the ATLAS experimental cross section $\hat{\sigma}_{\text{EXP}}$ (cf. Eq. (5)). The two cross sections σ_{EXP} and σ_{B} are listed in Table 2. The other background cross section $\sigma_{\text{B}}^{\text{gg}}$ takes only into account the non-resonant $gg \rightarrow 4l$ process and is computed by multiplying the bin size with the average differential cross section $(d\sigma_{\text{B}}^{\text{gg}}/dE)$ in each bin; see Ref. [20].

Bin [GeV]	$\hat{\sigma}_{\text{EXP}}$ [fb]	σ_T [fb]	χ^2
555-585	0.003 ± 0.060	0.048	0.56
585-620	0.105 ± 0.073	0.056	0.45
620-665	0.121 ± 0.078	0.123	0.00
665-720	0.152 ± 0.075	0.152	0.00
720-800	-0.067 ± 0.050	0.002	1.90
800-900	0.062 ± 0.055	0.004	1.11

TABLE 4: Comparing the experimental cross section in Table 3 with the theoretical Eq. (3) for the optimal set of parameters $M_H = 677$ GeV, $\Gamma_H = 21$ GeV, $\sigma_R = 0.40$ fb.

$\nu \sim 5.24 \pm 0.45$, and integrating the various contributions to Eq. (3) within each energy bin, a fit to the data gives $M_H = 677^{+30}_{-14}$ GeV, $\Gamma_H = 21^{+28}_{-16}$ GeV, and $\sigma_R = 0.40^{+0.62}_{-0.34}$ fb. The comparison for the optimal parameters is shown in Table 4.

The quality of our fit is good, but error bars are large. Yet, by restricting again to the central values, there is good agreement with our expectations. Indeed, by rescaling the partial width from $\Gamma(H \rightarrow ZZ) \sim 1.6$ GeV to 1.55 GeV (for M_H from 700 to 677 GeV), and fixing $\langle\Gamma_H\rangle = 21$ GeV, we find a branching ratio $B(H \rightarrow ZZ) \sim 0.073$. For the theoretical value $\sigma_{\text{ggF}}(pp \rightarrow H) \sim 1100$ fb of Ref. [15] (at $M_H = 677$ GeV), this would then imply a theoretical peak cross section $(\sigma_R)^{\text{Theor}} = 1100 \times 0.073 \times 0.0045 \sim 0.36$ fb, which only differs by 10% from the central value $\langle\sigma_R\rangle = 0.40$ fb of our fit. Moreover, from the central values of the fit $\langle\sigma_R\rangle = 0.40$ fb and $\langle\gamma_H\rangle = 0.031$, we find $\langle\sigma_R\rangle \times \langle\gamma_H\rangle \sim 0.012$ fb, again in good agreement with our Eq. (2).

Summarising: from the two ATLAS papers Refs. [17] and [19], we find consistent indications of a new resonance in our theoretical mass range $(M_H)^{\text{Theor}} \sim 690(30)$ GeV. By comparing with Ref. [19], we identify more precisely the non-resonant background $gg \rightarrow 4l$, which can interfere with a second resonance H produced via gluon-gluon fusion. Thus, the determinations obtained with our Eq. (3) are more accurate, from a theoretical point of view. In practice, there is not too much difference with the previous Refs.[12, 13] based on the ggF-low events of [17]. Indeed, the two mass values $(M_H)^{\text{EXP}} = 677^{+30}_{-14}$ GeV vs. $(M_H)^{\text{EXP}} = 706(25)$ GeV and the two decay widths $\Gamma_H = 21^{+28}_{-16}$ GeV vs. $\Gamma_H = 29 \pm 20$ GeV are well consistent within their uncertainties. Most notably, our crucial correlation Eq. (2) is well reproduced by the central values of the fits to the two sets of data.

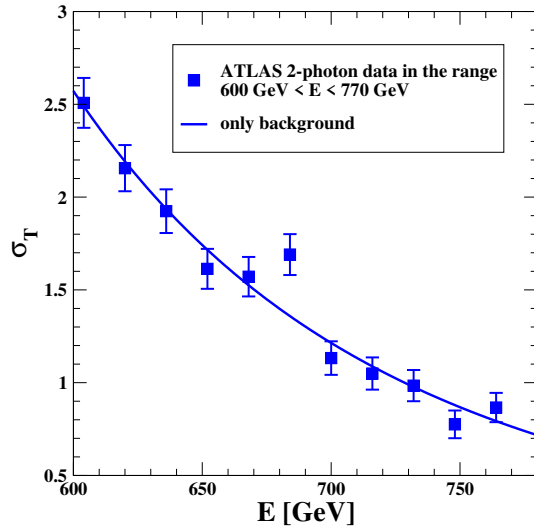


FIGURE 3: The fit with Eq. (3) and $\sigma_R = 0$ to the ATLAS data [21] shown in Table 5, transformed into cross sections in fb. The χ^2 value is 14, with the background parameters $A = 1.35$ fb and $\nu = 4.87$.

μ	604	620	636	652	668	684	700	716	732	748	764
N	349	300	267	224	218	235	157	146	137	108	120

TABLE 5: The ATLAS number $N = N(\gamma\gamma)$ of events, in bins of 16 GeV and for luminosity 139 fb^{-1} , for the range of invariant mass $\mu = \mu(\gamma\gamma) = 600 \div 770$ GeV. These values were extracted from Fig. 3 of Ref. [21], because the relevant numbers are not reported in the companion HEPData file.

2.2. The ATLAS high-mass $\gamma\gamma$ events

References [12, 13] also considered the invariant-mass distribution of the inclusive diphoton events observed by ATLAS[21]; see Table 5. By parametrising the background with a power-law form $\sigma_B(E) \sim A \times (685 \text{ GeV}/E)^\nu$, a fit to the data in Table 5 gives a good description of all data points, except for a sizable excess at 684 GeV (estimated by ATLAS to have a local significance of more than 3σ); see Fig. 3. This isolated discrepancy shows how a (hypothetical) new resonance might remain hidden behind a large background nearly everywhere. For this reason, apart from the mass $M_H = 696(12)$ GeV, the total decay width is determined very poorly, namely $\Gamma_H = 15^{+18}_{-13}$ GeV, but still consistent with the other loose determinations from the 4-lepton data. In Fig. 4 we show three fits with the full Eq. (3), for $\Gamma_H = 15, 25,$ and 35 GeV.

2.3. ATLAS and CMS ($b\bar{b} + \gamma\gamma$) events

The ATLAS and CMS Collaborations have also searched for new resonances decaying, through two intermediate $h(125)$ scalars, into a $b\bar{b}$ quark pair and a $\gamma\gamma$ pair. In particular, in Ref. [22] one considered the cross section for the full process

$$\sigma(\text{full}) = \sigma(pp \rightarrow X \rightarrow hh \rightarrow b\bar{b} + \gamma\gamma). \quad (6)$$

For a spin-zero resonance, the 95% upper limit $\sigma(\text{full}) < 0.16$ fb, for an invariant mass of 600 GeV, was found to increase by about a factor two, up to $\sigma(\text{full}) < 0.30$ fb in a plateau $650 \div 700$ GeV, and then to decrease for larger energies; see Fig. 5. The local statistical significance is modest, about 1.6σ , but the relevant mass region $M_X \sim 675(25)$ GeV is precise and agrees well with our prediction. The analogous ATLAS plot is depicted in Fig. 6 (which is the same

Fit with interference of a background + resonance

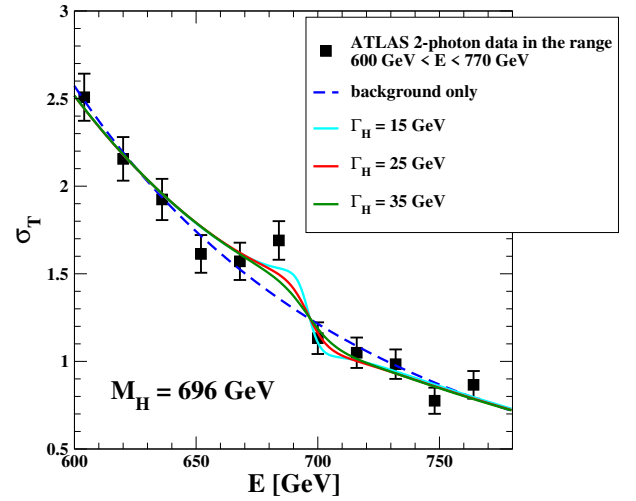


FIGURE 4: Three fits with Eq. (3) to the ATLAS data [21] in Table 5, transformed into cross sections in fb. The χ^2 values are 7.5, 8.8, 10.2, for $\Gamma_H = 15, 25,$ and 35 GeV, respectively.

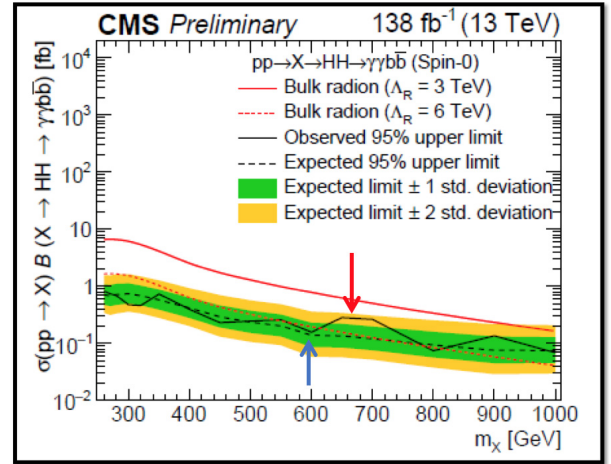


FIGURE 5: Expected and observed 95% upper limit for the cross section $\sigma(pp \rightarrow X \rightarrow h(125)h(125) \rightarrow b\bar{b} + \gamma\gamma)$ observed by the CMS Collaboration [22].

as Fig. 15 of the ATLAS paper Ref. [23]). Again, one finds a modest 1.2σ excess at 650 (25) GeV immediately followed by a 1.4σ defect, which could indicate a negative above-peak ($M_H^2 - s$) interference effect as found in the ATLAS 4-lepton data.

2.4. CMS-TOTEM $\gamma\gamma$ events produced in pp diffractive scattering

The CMS and TOTEM Collaborations have also been searching for high-mass photon pairs produced in pp diffractive scattering, i.e. when both final protons are tagged and have large x_F . For our scope, the relevant information is contained in Fig. 7, taken from Ref. [24]. In the range of invariant mass 650 (40) GeV and for a statistics of 102.7 fb^{-1} , the observed number of $\gamma\gamma$ events is $N^{\text{EXP}} \sim 76(9)$, to be compared with an estimated background $N_B \sim 40(9)$. In the most conservative case, viz. $N_B = 49$, this is a local 3σ effect and is the only statistically significant excess in the plot.

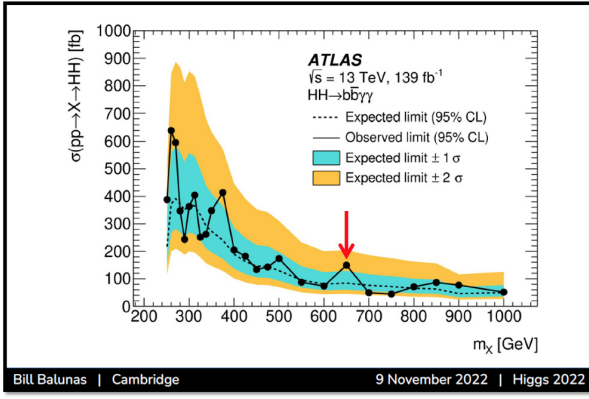


FIGURE 6: Expected and observed 95% upper limit for the cross section $\sigma(pp \rightarrow X \rightarrow h(125)h(125))$ extracted by the ATLAS Collaboration from the final state $(b\bar{b} + \gamma\gamma)$. The figure is taken from the talk given by Bill Balunas at Higgs-2022 and is the same as Fig. 15 of the ATLAS paper Ref. [23].

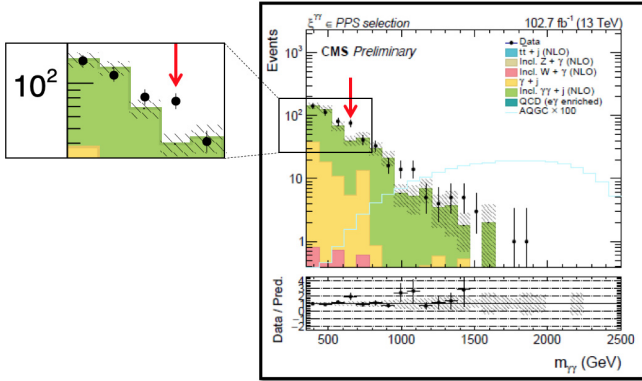


FIGURE 7: The $\gamma\gamma$ events produced in pp diffractive scattering [24]. In the bin 650 (40) GeV, one finds $N^{\text{EXP}} \sim 76(9)$, compared to an estimated background $N_B \sim 40(9)$.

3. SUMMARY AND CONCLUSIONS

Let us summarise our review of LHC data:

- i) The ATLAS ggF-like four-lepton events [17] reported in Table 1 show a definite excess-defect sequence, suggesting the existence of a new resonance. The same pattern is also visible in the ATLAS cross section [19]; see Table 2 and the $\Delta\sigma$ in Fig. 2. The combined statistical deviation in the latter analysis is at the 3σ level and indicates a resonance mass $M_H = 677^{+30}_{-14}$ GeV.
- ii) Observing the $+3\sigma$ excess at 684 (16) GeV in the inclusive ATLAS $\gamma\gamma$ events [21], a fit to these data was performed in Refs. [12, 13]. The resulting mass is $M_H = 696$ (12) GeV.
- iii) An overall $+2\sigma$ effect in the $(b\bar{b} + \gamma\gamma)$ channel is obtained by combining the excess of events observed by ATLAS at 650 (25) GeV and the corresponding excess observed by CMS at 675 (25) GeV.
- iv) A $+3\sigma$ excess is present at 650 (40) GeV in the distribution of CMS-TOTEM $\gamma\gamma$ events produced in pp diffractive scattering.

By combining the above determinations i-iv), the resulting estimate $(M_H)^{\text{EXP}} \sim 682$ (10) GeV, is in very good agreement with our

expectation $(M_H)^{\text{Theor}} = 690$ (30) GeV. We stress again that, when comparing with a definite prediction, one should look for deviations from the background nearby, so that local significance is not downgraded by the so called “look elsewhere” effect. Therefore, since the correlation of the above measurements is small, the combined statistical evidence for a new resonance in the expected mass range is far from negligible and close to (if not above) the traditional 5σ level. We also emphasise that the determinations i) and ii) above were obtained by fitting the numerical data reported in Refs. [17, 19, 21] to the general expressions Eqs. (3) and (4). This is very different from comparing with other Beyond-Standard-Model scenarios (such as supersymmetry, extra-dimensions, ...), whose exclusion limits assume built-in constraints (such as mass-width and/or mass-couplings relations) that are not valid in our approach. For this reason, we look forward to new precise data on which we can carry out the same general analysis as with the ATLAS papers [17, 19, 21].

References

- [1] G. Aad *et al.* [ATLAS Collaboration], Phys. Lett. B **716**, 1 (2012).
- [2] S. Chatrchyan *et al.* [CMS Collaboration], Phys. Lett. B **716**, 30 (2012).
- [3] V. Branchina, E. Messina, Phys. Rev. Lett. **111**, 241801 (2013).
- [4] E. Gabrielli, *et al.*, Phys. Rev. D **89**, 015017 (2014).
- [5] G. Degraess *et al.*, JHEP **08**, 098 (2012).
- [6] M. Consoli, L. Cosmai, Int.J.Mod.Phys. A **35**,2050103(2020).
- [7] M. Consoli, L. Cosmai, Symmetry **12**, 2037 (2020).
- [8] M. Consoli, Acta Phys. Polon. B **52**, 763 (2021).
- [9] M. Consoli, G. Rupp, arXiv:2308.01429 [hep-ph].
- [10] M. Consoli, L. Cosmai, Int.J.Mod.Phys.A **37**, 2250091 (2022).
- [11] M. Consoli, L. Cosmai, F. Fabbri, PoS **ICHEP2022**, 204 (2022).
- [12] M. Consoli, L. Cosmai, F. Fabbri, arXiv:2208.00920 [hep-ph].
- [13] M. Consoli, L. Cosmai, F. Fabbri, Universe **9**, 99 (2023).
- [14] <https://twiki.cern.ch/twiki/bin/view/LHCPhysics/CERNYellowReportPageBSMAt13TeV>.
- [15] <https://twiki.cern.ch/twiki/bin/view/LHCPhysics/CERNYellowReportPageAt13TeV>.
- [16] A. M. Sirunyan *et al.* [CMS Collaboration], JHEP **02**, 149 (2019).
- [17] G. Aad *et al.* [ATLAS Collaboration], Eur. Phys. J. C **81**, 332 (2021).
- [18] ATLAS Collaboration, <https://www.hepdata.net/record/ins1820316>.
- [19] G. Aad *et al.* [ATLAS Collaboration], JHEP **07**, 005 (2021).
- [20] ATLAS Collaboration, <https://www.hepdata.net/record/ins1849535>.
- [21] G. Aad *et al.* [ATLAS Collaboration], Phys. Lett. B **822**, 136651 (2021).
- [22] CMS Collaboration, arXiv:2310.01643 [hep-ex].
- [23] G. Aad *et al.* [ATLAS Collaboration], Phys. Rev. D **106**, 052001 (2022).
- [24] CMS and TOTEM Collaborations, arXiv:2311.02725 [hep-ex].